EARTHQUAKE SPECTRA

The Professional Journal of the Earthquake Engineering Research Institute

PREPRINT

This preprint is a PDF of a manuscript that has been accepted for publication in *Earthquake Spectra*. It is the final version that was uploaded and approved by the author(s). While the paper has been through the usual rigorous peer review process for the Journal, it has not been copyedited, nor have the figures and tables been modified for final publication. Please also note that the paper may refer to online Appendices that are not yet available.

We have posted this preliminary version of the manuscript online in the interest of making the scientific findings available for distribution and citation as quickly as possible following acceptance. However, readers should be aware that the final, published version will look different from this version and may also have some differences in content.

The DOI for this manuscript and the correct format for citing the paper are given at the top of the online (html) abstract.

Once the final, published version of this paper is posted online, it will replace the preliminary version at the specified DOI.

Seismic Performance of Nonductile Reinforced Concrete Frames with Masonry Infill Walls: II. Collapse Assessment

Siamak Sattar,[a] M.EERI and Abbie B. Liel,[b] M.EERI

This paper quantifies the collapse performance of a set of masonry-infilled reinforced concrete (RC) frame buildings that are representative of 1920s-era construction in Los Angeles, California. These building have solid clay brick infill walls, and vary in height (2-8 stories), wall configuration (bare, partially and fully-infilled frames) and wall thickness (1-3 wythes). The buildings' collapse behavior is assessed through dynamic analysis of nonlinear models. These models represent the walls by diagonal struts whose properties are developed from finite element analyses, as described in the companion paper, and represent beam-columns with lumped-plasticity models. The results indicate that the presence of infill walls can increase the risk of collapse. The most collapse prone of the buildings considered are those with strong, heavy infill walls, which induce large force demands in the frame elements. The partially infilled frames, which have a soft and weak first story, also perform poorly.

INTRODUCTION

Since the early 1900s, reinforced concrete (RC) frames with masonry infill walls have been a popular form of construction in earthquake-prone regions. Past earthquakes have caused severe damage to these structures including: partial or full failure of masonry walls; shear failure of columns; soft story mechanisms; and, sometimes, complete collapse (Bennett et al. 1996; Liel and Lynch 2012; Li et al. 2008; Moehle et al. 2006; Sezen et al. 2003). This damage can be attributed to 1) nonductile detailing of RC elements, *e.g.* inadequate transverse reinforcement and short lap splices; 2) brittle behavior of walls and interaction between walls and frame; and 3) torsional or vertical irregularities created by wall locations.

Previous research has shown that some nonductile RC frame structures have substantially

[a] University of Colorado-Boulder, 1111 Engineering Dr., Boulder, CO 80309. Currently: National Institute of Standards and Technology, 100 Bureau Dr., Gaithersburg, MD 20899.
[b] University of Colorado-Boulder, 1111 Engineering Dr., Boulder, CO 80309.

higher risks of earthquake-induced collapse than other buildings, potentially posing a seismic safety threat (Baradaran Shoraka et al. 2013; Liel et al. 2011). However, these studies did not examine buildings with masonry infill walls. The presence of infill walls has a significant impact on the seismic response of a RC frame building, increasing strength, stiffness and energy dissipation (relative to a bare frame), but, at the same time, introducing brittle failure mechanisms associated with wall failure and wall-frame interaction. Experiments have shown that some nonductile RC frames with infill walls may have reasonably good seismic performance (Stavridis et al. 2012). On the other hand, there are also reconnaissance studies that suggest that the infill can have a negative influence on RC frame performance. As such, the characteristics of infill walls that act to improve or worsen collapse risk, particularly in comparison to a RC frame that does not have infill walls, are unknown. The problem is compounded by the substantial variability of wall characteristics, frame characteristics, and plan and elevation configurations of these buildings. To provide context for interested readers, the Appendix describes selected previous reconnaissance, experimental and analytical studies examining masonry-infilled RC frames.

This study assesses the collapse risk of a set of older masonry-infilled RC frame buildings like those found in high seismic regions of the U.S.. The assessment is based on a set of 13 archetypical buildings that are designed according to 1920s-era practice in Los Angeles, California without seismic loads and without the benefit of seismic detailing. All of the buildings examined have solid brick walls, but with different thicknesses and configurations. As such, the paper explores how the presence of relatively strong brick walls affects the response of a regular frame with detailing representative of older California concrete buildings. Collapse performance is evaluated through repeated nonlinear time history analyses of each building. The buildings are modeled following the approach proposed in the companion paper (Sattar and Liel 2015).

ARCHETYPICAL BUILDINGS

CHARACTERISTICS AND CONFIGURATION OF ARCHETYPICAL BUILDINGS

RC buildings started to become common in Los Angeles and other high seismic areas in the U.S. at the start of the 20th century (Linares 2007). This popularity stemmed in part from the poor performance of non-engineered structures in the 1906 San Francisco earthquake, which motivated a move toward RC and steel buildings. In addition, construction of mid to

high rise buildings grew in downtown Los Angeles in the 1920s and 1930s due to the increased need for government and commercial offices (Linares 2007). These buildings were not typically designed to resist seismic loads and were built with what is now considered to be deficient detailing, in terms of the amount and configuration of reinforcement. Many of the RC and steel frame buildings from this era had unreinforced masonry infill walls.

Many of these structures are still in use, and only a small fraction have been retrofitted (Holmes et al. 2013). Data from Anagnos et al. (2010), who surveyed RC buildings built in the city of Los Angeles before 1980, are used to identify typical characteristics of older concrete buildings with and without infill walls. About 25% of the 1600 buildings surveyed are from the 1920s, the largest number from any single decade before 1980. The height distribution of the surveyed buildings indicates that most (> 85%) have 8 or fewer stories. Older concrete buildings are commonly used for industrial, commercial, or office purposes (accounting for 50% of the pre-1980 RC building stock).

On the basis of these observations, this study examines a set of 2, 4 and 8-story archetypical RC frame buildings with unreinforced masonry infill walls and office/ commercial occupancy that are representative of 1920s-era engineering practice in Los Angeles, as listed in Table 1. All buildings are 120 ft. by 72 ft. in plan. This geometry is consistent with typical dimensions reported by Faison et al. (2004). The archetypical buildings have 12 ft. story heights, which is in the range of 10-12 ft. reported as typical of older RC buildings (Bennett et al. 1996; Faison et al. 2004). Beam span lengths of 18-20 ft. are selected based on data from the same sources. The floor system is a 2.5 in. slab-joist system. Three different infill configurations are considered for each archetypical building: 1) fully-infilled, 2) partially-infilled, in which all stories, except the first, have infill walls, and 3) no infill (bare frame). Infill is assumed to be the same along every frame line.[1] Buildings with asymmetric distributions of infill walls resulting in plan irregularities are outside the scope of this effort.

MATERIAL PROPERTIES AND DESIGN OF RC FRAMES

The assumed material properties are representative of construction materials used in the 1920s. The compressive strength of concrete, f_c', is estimated to be 3000 psi for both columns and beams (ASCE/SEI 2013). The study assumes steel yield strength, f_y, of 33 ksi for

[1] The authors also examined buildings with highly punched interior walls, assuming walls had been removed in remodeling (Sattar 2013). These buildings are excluded from this paper for brevity.

longitudinal reinforcement in beams and transverse reinforcement in columns and beams, and 50 ksi for longitudinal reinforcement in columns (ASCE/SEI 2013; Stavridis 2009).

Table 1. Archetypical RC frame buildings with masonry infill walls: characteristics and seismic assessment results.

Building identifier*	No. of stories	Infill	No. of wythes of masonry infill	Pushover analysis results			IDA results	
				T_1 (sec)	Base shear strength (kips)	RDR** at 20% strength loss	Median collapse capacity S_{di} (in)***	% Change in median S_{di} w.r.t bare frame of the same height
Bare Frames								
2BW0	2	No	n/a ("Bare")	0.4	113	3.3	3.8	n/a
4BW0	4	No	n/a	0.7	122	2.1***	3.6	n/a
8BW0	8	No	n/a	1.1	164	2	4.7	n/a
Frames with "Strong" Walls								
2FW3	2	Full	3 ("Strong")	0.12	366	0.4	3.1	-18
2PW3	2	Partial	3	0.39	120	1.5	2.1	-44
4FW3	4	Full	3	0.24	469	0.3	1.9	-47
4PW3	4	Partial	3	0.5	191	0.6*****	2.1	-42
8FW3	8	Full	3	0.44	610	0.5	3.5	-26
8PW3	8	Partial	3	0.56	473	0.6****	2.7	-42
Frames with "Weak" Walls								
2FW1	2	Full	1 ("Weak")	0.18	270	0.5	2.8	-25
2PW1	2	Partial	1	0.37	120	1.5	2.7	-29
4FW1	4	Full	1	0.3	335	0.3	2.3	-35
4PW1	4	Partial	1	0.46	189	0.8	2.0	-45

* The building identifier reports number of stories, followed by a letter indicating the infill configuration (B- bare; F– fully-infilled; P- partially-infilled), followed by W and the number of wythes in each wall.
** Roof drift ratio, computed as the roof displacement divided by building height, presented as a percentage.
*** For all buildings S_{di} is computed using a common period and yield displacement to ensure results are comparable across buildings.
**** RDR at 15% loss of strength (last converged step of pushover).
***** RDR at 5% loss of strength (last converged step).

The frames are designed based on the working stress design methodology presented in the 1927 Uniform Building Code (ICBO 1927) and RC design texts published around that time (Turneaure and Maurer 1914, 1935). Earthquake forces are not considered in the design. Wind forces are calculated based on the requirements of the 1927 UBC (ICBO 1927), but the designs are governed by the combination of dead (from frame elements, masonry walls, floor system, ceilings, and parapets on the roof perimeter) and live loads. An unbalanced distribution of live loads is considered, but does not govern. Following 1920s design practice, approximate relationships from the 1927 UBC (ICBO 1927) rather than computer analysis are used to quantify load effects (moments) in beams and columns. These moment demands

are compared to allowable stress limits for the various components in concrete frames defined by the same document (ICBO 1927).

For each building, a typical four-bay two-dimensional frame oriented in the short direction is designed, as shown in Figures 1 and 2. The beam design in Figure 2 applies at non-roof levels of all of the archetypical buildings. The use of bent bars for shear reinforcement in beams and widely spaced transverse reinforcement in columns is supported by review of design documents and other materials from the 1920s (Holmes et al. 2013; Turneaure and Maurer 1914, 1935). Some of the beam bottom reinforcement is assumed to continue through the column, following anchorage recommendations from that time (Turneaure and Maurer 1914). Beams and columns in all frames are designed for the masonry walls' dead load, but infill configuration does not otherwise affect the design. The effect of biaxial bending on the design of corner columns is neglected. For more details about the design process, see Sattar (2013).

MATERIAL PROPERTIES AND CONFIGURATION OF MASONRY WALLS

The properties of the masonry infill walls are consistent with 1920s-era southern California buildings. Clay brick was the most common type of masonry at that time (FEMA 1998; Hamburger and Meyer 2006), with cement-lime-sand mortar (Stavridis et al. 2012). Typical 1920s-era brick sizes are taken from Kariotis (1991), who surveyed two Los Angeles infilled RC frames. Stang et al. (1929) tested bricks from 1920s, finding an average compressive strength, f_c', of 3280 psi. The average mortar thickness of 0.5 in. reported by Kariotis (1991) and Stang et al. (1929) is adopted here as typical.

The city of Los Angeles sampled and tested clay brick masonry walls from four pre-1934 unreinforced masonry buildings in the 1970s (Schmid et al. 1978). These tests are used to quantify the expected shear and compressive strength of the infill walls. The compression tests produced strengths of 400-500 psi (Schmid et al. 1978). Schmid et al. (1978) further proposed that the ultimate shear stress of the masonry wall, *V,* depends on the vertical stress in the wall, *P,* where:

$$\mathrm{V(psi)} = 1.2[30 + \mathrm{P\ (psi)}] \quad (1)$$

In infilled RC frames of this era, the exterior frames were often infilled with two or more wythe walls (ATC 2010; Hamburger and Meyer 2006). Two sets of assumptions are made here about the number of wythes, as reported in Table 1. For buildings with "strong" walls,

the infill is composed of a three-wythe wall; for the buildings with "weak" walls, the infill consists of a single-wythe wall. The effect of plaster on the walls is not considered. For simplicity, openings in infill walls are neglected.

Figure 1. Design of interior and exterior columns for archetypical buildings. Note that the 2-story and 4-story buildings are identical to the top two and four stories of the 8-story building, respectively, as shown.

Figure 2. Design of beams at an arbitrary floor level for archetypical buildings. Roof beams are designed for slightly lower gravity loads.

NONLINEAR SIMULATION MODELS

OVERVIEW

The collapse assessment of the archetype buildings in this study employs the strut modeling enhanced by finite element analyses (FE-enhanced strut modeling) approach developed by Sattar and Liel (2015). The strut models represent the 2D frame for nonlinear time history analysis, employing models of beams, columns, joints and struts that represent the response of the infill walls. Figure 3 illustrates the key properties of these models.

STRUT MODELS FOR MASONRY INFILL WALLS

As shown in Figure 3, infill walls are represented by two compression struts activated in each direction, in order to mimic the effect of infill-frame interaction on the distribution of forces in the frame elements such that shear failure at top of the columns can be simulated (Sattar and Liel 2015). The properties defining the struts are obtained by extracting the force-displacement response of the infill in the diagonal direction from FE model results.

Figure 3. Key elements of the nonlinear strut model of a 2D frame, illustrated for the 4-story buildings. The details of the model are shown for only one bay, but apply throughout.

Finite Element Models

The DIANA FE software is used to develop single-bay, single-story models of the frame and infill to predict the force-displacement response of the walls (DIANA 2011). A unique FE model is created for an interior bay of each story of each archetypical building, accounting for the member sizes and reinforcement, etc. of that distinct story. The material models and element types used in modeling the masonry infilled frames in the FE models are the same as those explained in the companion paper (Sattar and Liel 2015). The FE model

requires the definition of material properties for the brick and mortar. For the buildings examined in this study, for which in situ test data are not available, as is the typical case in practice, these parameters are obtained from four sources: 1) parameters (denoted *) defined directly in the literature; 2) parameters (§) defined indirectly based on the first group of parameters by conducting a calibration process in DIANA; 3) parameters (¶) computed based on parameters in first or second group, using available equations relating different parameters for a given material together; and 4) parameters (†) with no available data.

Model Properties for Mortar

The parameters defining the model for the mortar interface in DIANA are listed in Table 2. To determine the normal stiffness modulus of the interface $K_{nn}{}^{\S}$, a wallette model is made in DIANA. The mortar K_{nn} is calibrated such that the elastic slope of the wallette compressive stress-strain response equals the expected Young's modulus value of the masonry, *E*. *E* is assumed to be $750f_m'$ as proposed by ICBO (1997). The shear stiffness modulus of the interface, $K_{ss}^{\P}$, is computed as $K_{ss} = K_{nn}/2(1+v)$.

The compressive strength of the infill is usually governed by the compressive strength of the mortar joint, which is the weakest part of the wall. To obtain the compressive strength of the mortar, $f_c'^{\S}$, the same DIANA wallette model with elastic bricks is compressed. The value of the mortar f_c' is varied until the compressive strength of the wallette, $f_m'^{*}$, becomes 500 psi, as predicted by the literature review for the era and type of walls of interest. The tensile strength of the mortar, $f_t^{\P}$, is taken to be 6% of f_c' (Rao 2001). The mortar mode-I fracture energy, G_f^{I*}, is interpolated from the splitting test data from Wittmann (2002), which showed that G_f^I is 0.7-0.9 psi-in for concrete with f_t of 28-55 psi. Compressive fracture energy, $G_{fc}^{\P}$, is determined by a relationship proposed by Nakamura and Higai (2001).

Shear properties of the mortar are defined next. The cohesion parameter, $C^{\S}$, is the shear strength of mortar under zero vertical load. C is determined using a model composed of two elastic bricks and one layer of mortar, and lateral, but no vertical load. C is calibrated such that the shear strength of the modeled specimen becomes equal to the prediction from Equation (1) with no vertical load. The internal friction angle, $\Phi_i{}^{*}$, is defined as the slope of the line presented in Equation (1), and defines the initial relationship between vertical stress and shear capacity in the model. The residual friction angle, $\Phi_r{}^{\dagger}$, is taken as $0.9\Phi_i$, based on experimental results from Mehrabi (1994). The mode-II fracture energy, $G_f^{II\P}$, is computed

based on a relation proposed by Lotfi and Shing (1994), which relates the mode-I and mode-II fracture energies as $G_f^{II} = 10\ G_f^I$.

There is a lack of available data for dilatancy angle, $\Psi^{\dagger}$, confining normal stress, $\sigma_c{}^{\dagger}$, softening parameter, $\delta^{\dagger}$, and relative plastic displacement at peak compressive strength, $\kappa_p{}^{\dagger}$. These values were adopted directly from those used in the companion study (Sattar and Liel 2015), even though the mortar is slightly different in that case.

Adjustments are made from the values in Table 2 to represent head joints and wall-to-frame joints, which are weaker than the bed joints. This study uses the ratio between the stiffness of the head joint and wall-to-frame joint to the bed joint of 0.8 reported by (Mehrabi 1994). This value is used to reduce the normal and shear stiffness, strength, cohesion, and friction angle parameters of the head and wall-frame joints from the respective bed joint properties. The mortar properties for the single-wythe wall are assumed to be the same as the three-wythe wall, but with smaller out-of-plane thickness.

Table 2. Interface (mortar) properties in FE models.

Para-meter	K_{nn} (lb/in^3)	K_{ss} (lb/in^3)	C (psi)	Φ_i (deg)	Ψ (deg)	Φ_r (deg)	σ_c (psi)	δ	f_t (psi)	G_f^I (psi-in)	G_f^{II} (psi-in)	f'_c (psi)	G_{fc} (psi-in)	κ_p (in)
Description	Normal stiffness modulus	Shear stiffness modulus	Cohesion	Internal friction angle	Dilatancy angle	Residual friction angle	Confining normal stress	Dilatancy degradation coefficient	Tensile strength	Fracture energy for Mode-I	Fracture energy for Mode-II	Compressive strength	Compressive fracture energy	Relative plastic displacement at peak compressive strength
Source type	§	¶	§	*	†	†	†	†	¶	*	¶	§	¶	†
Inter-face	100000	43103	36	50	0.29	45	-150	2	31	0.72	7.21	515	92.7	0.006

Model Properties for Brick, Concrete and Steel

Table 3 presents the modeling parameters for the total strain crack model used to represent the clay bricks. This material model combines tensile and compression yield surfaces to capture the tensile cracking and compressive crushing that can occur in bricks. $f_c'^{*}$

of the bricks is based on the test results reported previously (Stang et al. 1929). The tensile strength, f_t¶, of the bricks is assumed to be 10% of f_c' or 300 psi (Drysdale et al. 1999). G_f^{I}* is taken as the average of experimental values reported by Van der Pluijm (1992) and Rao (2001) for bricks with f_t of 300 psi. The compressive fracture energy, G_c¶, of the bricks is computed using Nakamura and Higai (2001)'s equation. The brick's Young's modulus, E§, and Poisson's ratio, v§, match well with values for clay bricks reported in Lourenco (1996).

Table 3 presents the modeling parameters for the concrete in the FE representation of the concrete in the frame, which is also modeled with a total strain crack model. The compressive strength, f_c'*, is based on the literature review presented earlier. E¶ and f_t¶ are computed from f_c' based on standard relationships (ACI 2008). G_c¶ is computed from f_c' as proposed by Nakamura and Higai (2001). G_f^{I} ¶ is obtained from the same authors, who proposed that $G_c=250G_f^{I}$. Frame reinforcing steel is modeled with elastic-hardening-plastic material model. The yield stress, f_y*, of the steel is based on the assumed grade of steel. The ultimate stress, f_u*, of the steel is taken as 1.1 times the yield stress (Linares 2007).

Table 3. Brick and concrete properties in FE models.

Parameter	E (Ksi)	ν	f_t (psi)	G_f^I (psi-in)	f'_c (psi)	G_c (psi-in)
Description	Young's modulus	Poisson ratio	Tensile strength	Fracture energy for Mode-I	Compressive strength	Compressive fracture energy
Source type	§	§	¶	*	*	¶
Brick	2000	0.16	300	0.44	3000	224
Source type	¶	*	¶	¶	*	¶
Concrete	3122	0.16	329	0.89	3000	224

Extraction of FE Results to Define Strut Models

Eight distinct single-story single-bay FE models are required to represent each of the different stories in buildings with three-wythe walls; only four models with single-wythe walls are needed since the tallest such building considered has four stories.[2] Each single-bay single-story model has the frame element sizes and reinforcement of the story of interest. FE models of an interior bay are used to determine strut properties for both interior and end

[2] Recall that the 2- and 4-story buildings are identical to the top two and four stories, respectively, of the 8-story building, so the same FE models can be used to predict wall strut properties for both cases.

(exterior) bays for simplicity. Expected gravity loads are applied to each model. These loads are applied in the same sequence as in construction practice: the frame and floor system are built first, these loads are applied to the model, and the infill wall with its dead load is subsequently inserted (Cavaleri et al. 2004). Since the beam has already deflected under the dead load of the floor and frame system before the infill is installed, the infill carries only the vertical forces from loads applied after it is inserted, such as load of the ceiling and live load, and the weight of the wall of the floor immediately above. In the U.S., the frame tends to be tightly infilled on all sides, so infill is in direct contact with the frame (ATC 2010; FEMA 1998), and will take some of the gravity loads.

Once gravity loading is applied, each single-bay single-story FE model is subjected to static, monotonically increasing lateral displacements applied at the top of the model. The models were pushed past the peak strength and as far as solution convergence allows (Sattar and Liel 2015). Figure 4 illustrates the response of two of the FE models. The failure mechanism of the top story with three-wythe walls is characterized by diagonal step-cracking, as shown in Figure 4a. The top story with single-wythe walls experiences bed joint sliding and some distributed step-cracking pattern in the infill, as shown in Figure 4b. This difference in the failure modes is observed in Mehrabi (1994)'s experiments, and occurs due to the variation in the relative strength and stiffness of the frame and infill between the two cases.

Figure 4. Response of two of the FE models under monotonic loading, showing the deformed shape and crack pattern in the top story of archetypical buildings with: (a) three-wythe walls, and (b) single-wythe walls. The deformed shapes are shown immediately after peak strength is reached.

These results are used to extract the properties of the wall struts at each story, as described in the companion paper (Sattar and Liel 2015). Figure 5 shows the extracted force-displacement response for each of the eight stories in the buildings with three-wythe walls. Although the walls are the same at every story, Figure 5 indicates that increasing the vertical load on the FE models, in order to represent the lower stories in the taller buildings, leads to an increase in the observed strength of the infill response. Larger gravity forces in the FE model increase the shear strength of the mortar interfaces in the FE model as well as the size of the infill-frame contact length, which increase the strength of the wall. Figure 5 also shows that increase of the vertical loads in the lower stories lead to an increase in the stiffness and a reduction in ductility of the infill response. However, these trends may not be observed

between any two selected stories, due to variation of the frame dimensions and wall failure mechanisms at different stories. To simulate walls in the strut model, a multi-linear backbone is fitted to the extracted force-displacement responses at the appropriate story (Sattar 2013), an example of which is provided in Figure 5.

The response of the FE model is also used to estimate the contact length between the frame and infill, defining where the strut is connected to the frame elements in Figure 3. Since the FE models stop converging before the residual strength of the wall is reached, the fitted response assumes the residual shear capacity of the wall remains constant at 50% of its peak strength based on Stavridis (2009). Due to lack of the available data on the cyclic response of brick walls, the cyclic deterioration of struts is neglected in this study.[3]

This modeling approach attempts to ensure that the strut model captures the expected response and failure mode of the infill under lateral loading. It is noteworthy to mention that, although these strut models benefit from the accuracy of the FE modeling, the FE models are based on a single-bay specimen and the deformation of the internal and external columns, and consequently the wall-frame interaction, may differ in a multi-bay infilled frame model. More research could further improve the quantification of residual strength and the cyclic deterioration parameters for infill walls. Further details regarding the models and their limitations are presented in Sattar and Liel (2015).

BEAM-COLUMN MODELS

A RC beam or column may experience different failure modes depending on features such as its axial load and transverse reinforcement, and the appropriate modeling strategy depends on the expected failure mode. Beam response is typically flexurally dominated. For columns, the ratio of flexural to shear strength, V_p/V_n, can be used to determine the expected failure mode, where, V_p is the shear force corresponding to the development of the flexural strength at the ends of the columns, and V_n is column shear strength. Following criteria similar to that defined by ASCE/SEI (2013), columns in bare frames with $V_p/ V_n \leq 0.6$ are simulated with the purely flexural response and columns with $V_p/ V_n \geq 0.8$ are simulated with a shear model. The shear model is appropriate for columns that fail directly in shear and for those that yield first and then fail in shear. Observations from past earthquakes show that RC columns in masonry-infilled frames are highly susceptible to shear failure (*e.g.* Stavridis et al.

[3] The companion paper (Sattar and Liel 2015) shows how cyclic response of the infill wall can be incorporated in the strut modeling approach where experimental data are available for calibration of deterioration properties.

2012; Li et al. 2008), so these are modeled with the shear-based approach regardless of their V_p/V_n ratios.

Figure 5. Diagonal force versus lateral displacement response of infill walls extracted from the FE model of the buildings with "strong" walls, showing the extracted response from the eight different models representing different stories. The multi-linear force-displacement response fitted to the response extracted from the FE model of the top story and used to define the strut properties is also shown.

The modeling scheme adopted to simulate the response of flexurally-dominated elements employs a concentrated plasticity approach in which an elastic element is modeled in series with rotational plastic hinges at the member ends. The plastic hinge backbones and hysteresis are modeled with the Ibarra et al. (2005) material. The parameters defining the response are computed from empirical equations proposed by Haselton et al. (2008) such that model properties vary with design and detailing characteristics of the component of interest. This approach has been used in previous studies (Liel et al. 2011).

The features of the model used to simulate the response of the shear–critical and flexure-shear columns represent the state-of-the-art in phenomenological column shear failure models. This kind of model has been used by other researchers (Baradaran Shoraka et al. 2013; Elwood 2004), but has not previously been used in conjunction with the detailed wall models to represent infilled frames. Before shear failure occurs, the elastic element and rotational hinges dominate the response, as described above. To represent columns failing in flexure-shear, Elwood (2004) defines a failure surface that predicts when shear failure occurs as a function of shear force and deformation in the column. In order to capture columns that fail in shear before yielding, the Elwood model is modified by adding another shear failure surface based on the shear strength equation proposed by Sezen and Moehle (2004). Shear failure in a column initiates when the column response hits either limit surface. After shear failure, the shear spring takes on a negative slope to capture the strength degradation in a RC column after initiation of shear failure (Baradaran Shoraka and Elwood 2013). The column model also captures the potential loss of vertical bearing capacity (axial) failure that may occur after shear failure using the column axial failure model developed by Elwood (2004). In the model, shear failure is represented in an aggregate sense for each column by a shear spring at the top of each column. As a result, the local deformation patterns are only correctly observed if the shear failure occurs at the top of a column, but this is not expected

to significantly affect the collapse capacity assessments due to load reversals in dynamic analysis.

OTHER MODEL CONSIDERATIONS

Previous research is used to determine the level of damping to assign in the models. Hashemi and Mosalam (2007) performed shake table tests on a RC frame with clay brick infill walls, showing that the presence of the infill can increase the damping ratio of the representative linear model by 1.25 to 3 times, depending on the level of shaking. Cook (1985) also reported that the damping ratio of masonry infilled concrete frames varies from 5% at service load to 16% at ultimate load. Based on these findings, the infilled frame models are assumed to have 8% Rayleigh damping in the first and the third modes. This damaging is assigned only to the elastic elements of the frame and the struts. Additional damping may come from the hysteresis of the frame elements. However, the infilled frame models do not experience many cycles because brittle column shear failure occurs at a relatively small drift ratios so the contribution of hysteretic energy dissipation is low. The bare frames are modeled with 5% Rayleigh damping (also assigned only to elastic elements). Geometric nonlinearities (P-Δ) are considered in the analyses. Joints are modeled with finite size with elastic response. Although some older concrete frames have discontinuous or smooth beam bars in the joint, this effect is not considered.

OUT-OF-PLANE CONSIDERATIONS FOR INFILL WALLS

Out-of-plane failures of infill walls may have an important influence on response, particularly for slender walls. A number of models have been developed to predict out-of-plane strength of masonry infill walls. Flanagan and Bennett (1999) evaluated a group of available models, and proposed a modification to the Dawe and Seah (1989) empirical equations, which is used here to estimate the out-of-plane strength of the masonry infill walls. According to these calculations, the out-of-plane strength of the walls varies between 0.2 and 2.5 psi, depending on the material properties of the infill and infill geometry. The lower bound is associated with the single-wythe infill, which has lower out-of-plane resistance due to the smaller wall thickness. These values correspond to an equivalent acceleration, *i.e.* the acceleration that needs to be applied on the mass of the infill wall to induce an inertial force equal to the ultimate out-of-plane strength of the infill, of 0.9 (single-wythe walls) to 2.8g (three-wythe walls). There is limited experimental data for out-of-plane capacity of brick masonry walls, but available data finds clay brick walls have out-of-plane strengths ranging

from 8 to 19 psi (Gabrielsen and Kaplan 1997; Thomas 1953), indicating that the Flanagan and Bennett (1999) predictions for these walls likely underestimate the true strength.

Out-of-plane failure of the three-wythe walls is assumed to be highly unlikely under reasonable levels of ground shaking based on the evidence presented above. However, for the single-wythe walls, the equivalent acceleration may occur, as will be discussed in the results. Note that the interaction between the in-plane and out-of-plane response of the masonry infill wall is not considered in these estimates. Hashemi and Mosalam (2007) used FE models to suggest that increasing the out-of-plane forces, even if failure does not occur, reduces in-plane wall strength, but more experimental data is needed to refine these approaches.

COLLAPSE PERFORMANCE ASSESSMENTS

OVERVIEW

Collapse performance is assessed through the performance-based earthquake engineering methodology (Deierlein 2004), which provides a probabilistic framework for relating ground motion intensity to structural response and building performance through nonlinear time-history simulation. Incremental dynamic analysis (IDA) is used to analyze the seismic response of the strut model representation of the archetype buildings (Vamvatsikos and Cornell 2002). In IDA, a model is subjected to a ground motion record, and the structural response is simulated. The time-history analysis is repeated, each time increasing the scale factor on the input ground motion, until that motion causes collapse. This process is continued for a large set of ground motions. IDA can be used to produce fragility curves, which define the probability of experiencing a specific damage state, *e.g.* collapse, as a function of ground motion intensity. Due to the use of many ground motions in the analysis, the fragility functions quantify record-to-record variability in structural response.

The dynamic analysis uses 44 recorded ground motions from large crustal earthquakes recorded at moderate fault-rupture distances (*i.e.,* not near-fault conditions) (FEMA 2009). In this study, ground motion intensity is quantified by inelastic spectral displacement, S_{di}. S_{di} is the peak displacement of a single-degree-of-freedom oscillator with bilinear material properties subjected to the ground motion of interest (Tothong and Luco 2007). S_{di} depends on the oscillator's fundamental period, T_1, and the yield displacement, d_y, assuming a 5% post-yielding hardening stiffness ratio and 5% damping. The primary advantage of quantifying ground motion intensity with S_{di}, rather than spectral acceleration or another

measure, is its effectiveness in capturing both ground motion intensity and spectral shape (Tothong and Luco 2007). S_{di} captures the shape of the response spectra for periods greater than T_1 as the oscillator yields and the period elongates, causing it to respond to different regions of the spectra. This advantage is important because the spectral shape of records used in nonlinear time history analyses substantially impacts collapse assessments, yet it was infeasible to select ground motions with realistic spectral shapes for these analyses, since that process is inherently site and structure specific (Haselton et al. 2011). To compute S_{di}, T_1 and d_y can be quantified from pushover analysis. To facilitate comparison across buildings having different periods and yield drifts, S_{di} is in every case computed using the average T_1 and d_y of all buildings. As a result, the median collapse values for the different structures can be directly compared without further manipulation.

Collapse is defined to occur when a global lateral failure transpires at any story in the building. This definition of collapse is similar to that proposed by Baradaran Shoraka et al. (2013) and Shing (2013). Lateral failure is identified when the lateral capacity of a story degrades below the story's residual shear capacity, which is defined as 40% of the shear capacity of the undamaged story. The dynamically varying capacity of the story is monitored throughout the analysis, computed as the sum of the shear capacity of the columns and wall struts in that story (Sattar 2013).

METRICS OF COLLAPSE PERFORMANCE

Results of Static Pushover Analysis

Before dynamic analysis, static pushover analysis is conducted for all of the archetype buildings to quantify strength and deformation capacity. Pushover results are presented in Table 1 including: 1) the first-mode period (from eigenvalue analysis); 2) the base shear strength of the structure; and 3) the roof drift ratio at which 20% of the lateral strength of the structure has been lost, a measure of deformation capacity. Figure 6 illustrates pushover results for the 2-story buildings. All of the 2-story buildings fail in the first story, but the presence of infill substantially increases both the stiffness and the strength of the infilled frames.

Considering all the buildings, on average, the fully-infilled frames with strong walls have approximately 21 times larger initial stiffness and 3.6 times greater peak strength than the bare frames of the same height; the partially-infilled frames with strong walls have about 11

times larger stiffness and 2 times greater peak strength than the bare frames. However, the presence of infill in these frames also decreases the deformation capacity by 55-90%. The increase in strength and stiffness and reduction in deformation capacity of the infilled as compared to the bare frames are consistent with experiments (see Appendix). Unsurprisingly, the pushover results for the infilled frames with "weak" walls fall between the bare frames and the fully-infilled "strong" wall frames (on average 3.3 times stiffer and 1.9 times stronger than bare frames). The response of the frame partially-infilled with "weak" walls is almost identical to the partially-infilled frame with "strong" walls, because, for both buildings, the behavior is governed by the infill-free first story as can be expected for other partially-infilled buildings whose failure occurs in the first story.

The bare frames experience peak interstory drifts between 2% (8-story frame) and 3% (2-story frame) at the onset of the significant loss of strength in the pushover response. These deformation levels are in good agreement with experimental pushovers of nonductile frames by Mehrabi et al. (1996); modern ductile frames have much larger story drift capacities, *e.g.* >7% according to tests by Fardis (1996) and analyses by Haselton et al. (2011). The relatively high ductility of the older non-ductile frames is due in part to assumptions about design details, specifically 8 inch spacing of transverse reinforcement in columns, based on 1920s-era concrete design guidelines. Other buildings built in this era may have followed different detailing guidelines and have less ductility capacity.

Figure 6. Pushover results for 2-story archetype RC frame buildings with "strong" (three-wythe) and "weak" (single-wythe) brick infill walls.

Incremental Dynamic Analysis Results

The collapse risk of each of the RC frames is quantified from IDA results. Figure 7 illustrates the outcome of IDA for the 2-story bare and fully-infilled frames with "strong" walls, showing the relationship between ground motion intensity (S_{di}) and peak interstory drift ratio for each of the ground motions applied to the building model. These results can be summarized in the form of a collapse fragility curve, as shown in Figure 8. Table 1 reports the statistics of the collapse fragility curves for all of the archetypical buildings in terms of the median collapse capacity (quantified by S_{di}). The logarithmic standard deviations in collapse capacities are about 0.45 in all cases.

Figure 7. IDA results for the 2-story (a) bare frame (2BW0) and (b) fully-infilled frame (2FW3), showing interstory drift as a function of ground motion intensity for the different ground motions. (Colors relate to the more detailed results provided in Figure 9).

Figure 8. Collapse fragility curves for 2-story archetype RC frame buildings.

Effect of Infill

Results in Table 1 show that the bare frames consistently have better collapse performance (lower collapse probability) than the infilled frames for all building heights for the clay brick walls examined. On average, the median collapse capacities (S_{di}) of the fully-infilled and partially-infilled frames are 33% and 42% lower than the bare frames. Although this result may seem surprising, in fact the superior performance of the bare frame as compared to an infilled frame *with strong and heavy infill* is in agreement with the experience of the Hotel Montana structure in the 2010 Haiti earthquake (as described in the Appendix and Eberhard et al. 2013), and the greater percentage of red-tagged infilled versus non-infilled frames in the 2010 Canterbury earthquake (Kam et al. 2010).

These conclusions are a function of the strong, but heavy, walls considered and the shear criticality of the columns in a frame designed for wind and gravity loads. In the fully-infilled frames, the strong and stiff infill induces large shear forces first in the interior, then, exterior columns at the first story. The frame failure prevents the walls from reaching maximum capacity, and the story cannot carry more lateral loads. Figure 9 provides more detail about the model response of the infilled and bare frames, examining column shear force versus displacement response for a selected ground motion applied to both fully-infilled and bare frames. Figure 9 shows the column response at different excitation intensities for the selected ground motion, each shown with a different color (the same color also references to the overall IDA response on Figure 7). In Figure 9, the bare frame column yields in flexure at a relatively low shear force, but shows fairly ductile performance. Due to the change in shear distribution in the column, the columns in the fully-infilled frame take a larger force before failing, but then fail in a brittle shear mode. As a result, the fully-infilled frame collapses at lower intensity levels.

Figure 9. Example of detailed results obtained from IDA, showing column force versus interstory drift of an interior column in the first story at different intensity levels (S_{di}) in the 2-story (a) bare frame (2BW0) and (b) fully-infilled frame (2FW3). (Each color in Figure 9 is

obtained from the analysis represented by the same color in Figure 7.)

For most of the cases in Table 1, the partially-infilled frames have the worst collapse performance of the buildings analyzed. The poor collapse performance of the partially-infilled frames is driven by the large seismic mass coming from the heavy infill. This finding fits with engineering intuition and evidence from reconnaissance studies that partially-infilled frames are more susceptible to collapse due to soft/weak first stories (Sezen et al. 2003). However, for the 4-story buildings with strong walls, the partially-infilled frame actually has marginally better performance than the fully-infilled frame. In the 4-story case, the presence of the infill walls at the first-story increases mass relatively more than it increases stiffness and strength, so the partially-infilled frame, which also has greater deformation capacity at the first story, has slightly superior performance. The potential for the mass of strong walls to adversely affect performance is consistent with some of the reconnaissance studies described in the Appendix (Eberhard et al. 2013).

Effect of Wall Strength and Stiffness

The buildings with single-wythe "weak" walls show generally better collapse performance than the corresponding frames with three-wythe "strong" infill walls, such that the median collapse capacities of the frames with "weak" walls range from 91% to 126% of the frames with "strong" walls. The generally improved collapse performance occurs because the frames with single-wythe walls dissipate energy by failing before the frame. Since the walls are weaker and less stiff, they absorb lower earthquake forces, which has the impact of delaying column shear failure. However, the failure modes in frames with single-wythe walls in this study are still dominated by column-induced shear failure because even the single-wythe walls are relatively strong.

The significance, and even direction, of the effect of infill strength depends on the relative changes in stiffness, strength, and mass. For most of the archetypical buildings, the infill has a roughly proportional effect on mass and stiffness, such that the periods of the buildings with the two thicknesses of walls are similar.

Effect of Building Height

The collapse performance assessments yield median collapse capacities for the 8-story bare frames that are 24-31% higher than the 2 and 4-story bare frames. Unlike the 2 and 4-story buildings, which consistently fail in the first story, the 8-story buildings experience

distributed failure modes over multiple stories. This distribution stems from higher mode effects, as well as variation in strength and stiffness over the height as column sizes and reinforcement step down. The 8-story infilled frames also have greater collapse capacities than shorter infilled buildings, but the order of magnitude of the difference depends on the pair of buildings being compared. Post-earthquake observations for the Union School in the 2010 Haiti earthquake (Eberhard et al. 2013), as well as a 12-story building in the 1993 Guam earthquake (Moehle 2003), confirms the possibility of failure in a story other than the first story in an infilled frame.

Effect of Out-of-Plane Wall Failure

Calculations for out-of-plane wall strengths indicate that the single-wythe walls may fail out-of-plane, unlike the thicker three-wythe walls. In order to investigate the significance of neglecting this failure mechanism in the analysis, a "non-simulated" collapse mode is introduced (Liel et al. 2011). In this approach, the buildings with weak walls are judged to have collapsed if the peak ground acceleration (PGA) of the excitation exceeds the out-of-plane equivalent acceleration capacities for these walls. The collapse capacity statistics are recomputed as the minimum of the simulated (from the analysis) and non-simulated collapse capacities obtained for each ground motion. Results show that including the non-simulated collapse mode decreases the median collapse capacity of the buildings by 1-5%. More research is needed to incorporate out-of-plane wall failures in these frame models.

CONCLUSIONS

This study evaluates the collapse performance of nonductile RC frames with and without masonry infill walls, focusing on buildings that are representative of 1920s-era construction in Los Angeles. During this time, rapid population growth in southern California was accompanied by an increased need for mid to high-rise construction in downtown Los Angeles, adding substantially to the city's inventory of RC frames with masonry infill walls. It is well known that "nonstructural" infill walls may have both beneficial and deleterious impacts on seismic performance, increasing strength and stiffness, but inducing brittle shear failure in columns. This study examines how, on the balance, the presence of masonry infill walls impacts the collapse performance of these structures. The study is limited to buildings of the type constructed in California in the 1920s, having solid brick infill walls and regular plan configurations.

The study is conducted by designing and modeling a group of 13 RC frame buildings with clay brick masonry walls. The seismic response of each of these buildings is simulated using a FE-enhanced strut modeling approach. In the model, the walls are represented by struts with nonlinear force-displacement backbones, the properties of which have been obtained from FE modeling that incorporates expected brick and mortar properties and typical construction practices for the masonry walls. Beam-column models can capture the shear and subsequent axial failure of concrete columns. The collapse performance assessment is based on nonlinear time history analysis of the strut models of each building under 44 recorded ground motions.

Findings show that RC frames with brick masonry infill walls are more likely to collapse than bare frames with the same beam and column elements, due to the increased stiffness and mass coming from the strong masonry walls prematurely inducing brittle shear failure in columns. RC frames with weaker (single-wythe) brick walls show generally better performance than the frames with strong (three-wythe) brick walls because the frames with weak walls absorb lower earthquake forces, delaying shear failure of the columns. The partially-infilled weak-story frames generally perform worse than both the fully-infilled and bare frames because of the large seismic demands imposed on the first-story which does not have infill. These findings apply only to frames with design and configuration like those here, in that their response is governed by the infill-induced column shear failure due to the presence of relatively strong walls. Different collapse patterns would be observed in buildings with much weaker walls.

Future work should consider buildings with openings in masonry walls, and torsional irregularities created by the wall locations, since these conditions are common and contribute to collapse risk. The response may be quite different for RC frames with hollow clay tile infill, since these walls are much weaker and, hence, their failure is much less likely to cause shear failure in the RC columns. In this case, the walls may absorb energy protecting the columns. Buildings with different connections between the wall and the frame are also expected to behave differently.

ACKNOWLEDGMENTS

The authors gratefully acknowledge Maziar Partovi and Kesio Palacio, for providing technical support on DIANA modeling, as well as suggestions from Kenneth Elwood, Keith

Porter, and Guido Camata.

APPENDIX: REVIEW OF SEISMIC PERFORMANCE OF MASONRY INFILLED RC FRAMES

OBSERVED PERFORMANCE IN PAST EARTHQUAKES

This section describes reconnaissance studies from a number of recent earthquakes that have looked at damage to infilled RC frames, focusing on those that exemplify typical failure modes in these structures. Reports on the 1999 Kocaeli, Turkey earthquake (M_w 7.4), which destroyed almost 80,000 buildings and killed 17,000 people, documented typical failure modes of infilled RC frames. The main failure mechanisms reported involved diagonal cracking of the walls and flexural and shear cracking or failure of adjacent RC columns (EERI 1999). Sezen et al. (2003) also reported the concentration of drift in the weak and soft first story of frames in which infill was not present in the first story, which in some cases contributed to collapse. Observers in Kocaeli also concluded that the asymmetric distribution of infill walls was important contributor to collapse of RC buildings (Sezen et al. 2003). The frame and wall failure mechanisms in this earthquake are consistent with those reported in a number of other earthquakes (Kam et al. 2010; Li et al. 2008; Maheri 1990). The 1999 Tehuacan, Mexico earthquake (M_w 7.0) (Pestana et al. 1999) and 2008 Wenchuan, China (M_w 8.0) (Li et al. 2008) earthquakes confirmed the detrimental effect of lack of the infill walls in the first story on the collapse performance.

After the 2008 Wenchuan, China earthquake, which killed almost 70,000 people, a reconnaissance team observed that patterns of failure in RC frames depended on the type of infill (Li et al. 2008). Among RC frames with seismic detailing and hollow tile infill, damage was concentrated in the infill, because of the walls' low strength. However, among the RC frames with solid brick infill, damage was observed in both infill and frame, particularly if the infill was well-connected to the frame. The team concluded that asymmetric locations of infill walls and disregard of infill walls in the design process were among the primary contributors to the failure of buildings in this earthquake.

Observations from 2010 Haiti earthquake (M_w 7.0), which killed over 200,000 people, provides insight into the collapse response of infilled versus non-infilled RC frames. The USGS/EERI post-earthquake team (Eberhard et al. 2013) investigated the collapse of the

Hotel Montana, a five-story RC frame building constructed in 1946. One part of the building collapsed, as shown in

Figure 10a. This part of the hotel was constructed of an RC frame with concrete block infill walls. However, the hotel's lobby, which was also RC frame, but did not have extensive walls, remained intact (

Figure 10b). Eberhard et al. (2013) concluded that the heavy unreinforced masonry walls added weight but not much seismic resistance, causing the collapse of parts of the structure where significant infill was present. The report found that other building failures in Haiti could also be attributed to substantial weight coming from infill walls. The Haiti team further observed some other interesting failures. In particular, the three-story Union School, which had masonry infill walls in most bays, had nearly undamaged columns in the first and third stories, but substantial shear damage in columns in the second story. Although somewhat counterintuitive, another observed case of building failing in the second story is the 12-story infilled RC frame building in the 1993 Guam earthquake (M_w 8.1) (Moehle 2003).

Figure 10. Damage to the Hotel Montana in the 2010 Haiti earthquake, showing (a) collapse of the guest wing, constructed of a RC frame infilled with unreinforced masonry, and (b) the lobby, which lacked extensive walls and remained intact. Photos from Eberhard et al. (2013).

Post-earthquake building evaluations after the 2010 Canterbury, New Zealand, earthquake provide further insight into the comparative performance of masonry-infilled and bare frames (Kam et al. 2010). These evaluations, which utilized the ATC-20 procedure, showed that a higher fraction of masonry infilled RC frames were "red-tagged", as compared to the bare RC frames. On this basis, Kam et al. (2010) concluded that walls may negatively affect the performance of a RC frame.

Using their field experience as a guide, some engineers have suggested that masonry infilled RC frames do not tend to collapse, or perform better than bare frames. As this discussion shows, the story is actually more complex. Infilled frames have collapsed in the past and can perform better, worse or similarly to bare frames depending on their characteristics. The usefulness of post-earthquake observations in examining collapse performance is complicated by the fact that reconnaissance reports usually describe only damaged buildings and lack site-specific records of ground shaking intensity (Rossetto and Elnashai 2003).

OBSERVED PERFORMANCE IN EXPERIMENTS

A number of researchers have conducted cyclic and dynamic tests to assess the influence of masonry infill walls on the performance of concrete frames. Most of the experiments conclude that adding infill to the frame increases the strength and stiffness of the frame, but decreases deformation capacity (*e.g.* Anil and Altin 2007; Blackard et al. 2009; Al-Chaar et al. 2002; Fiorato et al. 1970; Hashemi and Mosalam 2007; Lee and Woo 2002; Mehrabi et al. 1996; Zarnic and Tomazevic 1988).

It is important to point out that most of these experiments have not studied the performance of the infilled frames in the highly nonlinear range, or directly compared infilled and bare frame response. One of the only tests examining collapse-level behavior of infilled frames is Stavridis et al. (2012). They tested a full-scale three-story, two-bay masonry-infilled RC frame, which is representative of a 1920s California building, on a shaking table. They reported shear failure of concrete columns and considerable, but repairable, damage to the structure at a ground motion intensity higher than the "maximum considered earthquake" ground motion at the selected site in Los Angeles. However, they did not compare to a bare frame response.

Of particular relevance here are those studies that compare the response of infilled and bare concrete frames. Mehrabi et al. (1996) conducted monotonic and cyclic in-plane tests on fourteen one-half-scale single-story frame specimens with different infill and frame configurations. They reported brittle shear failure in the columns as the dominant failure mode for the weak frames (*i.e.* frames that are not designed for earthquake forces) with strong walls. The drift at shear failure of the columns was in the range of 0.3% to 0.6% for weak frames. In comparison, the bare frame experienced flexural failure in columns, and reached a 5% drift ratio before experiencing substantial strength deterioration. Based on the comparison of different wall and frame types, they concluded that RC frames can benefit from the infill panel if the frame is designed and detailed for seismic forces. In another study, a full-scale four-story ductile RC frame building was tested dynamically with and without light infill panels at the European Laboratory for Structural Assessment (Fardis 1996). In these tests, bare, fully and partially-infilled frames were subjected to different excitation levels on a shaking table. Results of these experiments showed that the presence of infill reduced the drift demand in the fully-infilled frame. For the partially-infilled frames, drifts in the first story were amplified above those experienced in the bare frame, leading to damage

of the infill in the second story. None of the infilled frames was excited up to the collapse point. However, the bare frame did collapse, at an interstory drift ratio of 7%.

Lee and Woo (2002) also performed dynamic and static monotonic tests on one-fifth-scale two-bay three-story masonry infilled non-ductile concrete frames, observing better performance of bays with infill as compared to bare frame bays. This improvement was attributed to the fact that the increase in the inertial forces due to the existence of the infill is less than the increase in the strength associated with the infill. However, they did not excite the buildings up to the collapse, and the infilled frame building remained almost in the elastic range. They further hypothesized that when the response becomes nonlinear, the explosive behavior of strong walls can cause significant inelastic deformation demands on frame components, leading to failure.

OBSERVED PERFORMANCE IN ANALYTICAL STUDIES

This study builds most directly on recent analytical efforts to evaluate the seismic performance of masonry-infilled RC frames. Dymiotis et al. (2001) assessed the seismic vulnerability of two 10-story three-bay infilled RC frames of moderate ductility at "serviceability" and "ultimate" limit states using dynamic analysis. Their models utilized 2D lumped plasticity frame elements and homogenous four-node isoparametric nonlinear elements for infill. Findings showed that the bare frame is less likely to reach the ultimate limit state than the comparable infilled frame. Dolšek and Fajfar (2007, 2008) also evaluated the seismic performance of several 4-story masonry-infilled RC frames. The buildings were modeled with concentrated plasticity beam-columns and equivalent strut walls to conduct pushover analyses. These pushover results were used to define single-degree-of-freedom backbones for dynamically-based performance evaluation. In this analysis, the infilled frames had better performance than the bare frame. However, at high intensity excitation levels, the authors showed that infilled frames can experience a significant drop in lateral capacity after the walls fail. Madan and Hashmi (2008) evaluated the performance of 7 and 14-story RC frames with masonry infill representative of Indian construction. Walls were modeled with nonlinear struts. The buildings were subjected to near-fault ground motions, and performance-based seismic evaluation conducted using the capacity spectrum method and selected nonlinear dynamic time history analyses. Seismic damage, quantified in terms of deformation induced in the columns, was found to depend highly on the fraction of bays containing masonry infill in the first story, where more infill panels led to a better

performance of the structure. Finally, this study improves on our own previous attempt to assess the collapse risk of infilled RC frames through nonlinear dynamic analysis (Sattar and Liel 2010). That effort found that the infilled frame was less likely to collapse than the bare frame, due to the added strength from the masonry infill. However, the models were not able to capture important features of the wall-frame interaction or column shear failure.

REFERENCES

ACI, 2008. *ACI 318: Building Code Requirements for Reinforced Concrete*, American Concrete Institute, Farmington Hills, MI. 2008.

Al-Chaar, G., Issa, M., and Sweeney, S., 2002. Behavior of masonry-infilled nonductile reinforced concrete frames. *Journal of Structural Engineering*, 128(8), 1055–1063.

Anagnos, T., Comerio, M. C., Goulet, C., Steele, J., and Stewart, J. P., 2010. Development of a concrete building inventory: Los Angeles case study for the analysis of collapse risk. *Proc. of the 9th U.S. National & 10th Canadian Conference on Earthquake Engineering*, Toronto.

Anil, Ö., and Altin, S., 2007. An experimental study on reinforced concrete partially infilled frames. *Engineering Structures*, 29(3), 449–460.

ASCE/SEI., 2013. *Seismic rehabilitation of existing buildings*. ASCE, Reston, VA.

ATC., 2010. *Here Today-Here Tomorrow: The Road to Earthquake Resilience in San Francisco, ATC 52*. Applied Technology Council, Redwood City, California.

Baradaran Shoraka, M., and Elwood, K., 2013. Mechanical model for non-ductile reinforced concrete columns. *Journal of Earthquake Engineering*, 17(7), 937-957.

Baradaran Shoraka, M., Yang, T. Y., and Elwood, K. J., 2013. Seismic loss estimation of non-ductile RC buildings. *Earthquake Eng. & Structural Dynamics*, 42(2), 297–310.

Bennett, R. M., Flanagan, R. D., Adham, S., Fischer, W. L., and Tenbus, M. A., 1996. *Evaluation and analysis of the performance of masonry infills during northridge earthquake*. Oak Ridge, Tenn.

Blackard, B., Willam, K., and Mettupalayam, S., 2009. Experimental observations of masonry infilled RC frames with openings. *Thomas TC Hsu Symposium on Shear and Torsion in Concrete Structures*, 199–222.

Cavaleri, L., Fossetti, M., and PAPIA, M. (2004). "Effect of vertical loads on lateral response of infilled frames." Vancouver, B.C., Canada.

Cook, N. J., 1985. *The Designer's Guide to Wind Loading of Building Structures. In Building research establishment. Part 1*. Butterworths, London, United Kingdom.

Dawe, J. L., and Seah, C. K., 1989. Out-of-plane resistance of concrete masonry infilled panels. *Canadian Journal of Civil Engineering*, 16(6), 854–864.

Deierlein, G. G., 2004. Overview of a comprehensive framework for earthquake performance assessment. *Overview of a comprehensive framework for earthquake performance assessment,* PEER Rep. 2004/05, Berkeley, CA,, 15–26.

DIANA., 2011. *Finite element analysis*. TNO Building and Construction Research, Delft, Netherlands.

Dolšek, M., and Fajfar, P., 2007. Simplified probabilistic seismic performance assessment of plan-asymmetric buildings. *Earthquake Engineering & Structural Dynamics*, 36(13), 2021–2041.

Dolšek, M., and Fajfar, P., 2008. The effect of masonry infills on the seismic response of a four-storey reinforced concrete frame - a deterministic assessment. *Engineering Structures*, 30(7), 1991–2001.

Drysdale, R. G., Hamid, A. A., and Baker, L. R., 1999. *Masonry structures: behavior and design*. Prentice Hall, Boulder, Colorado, US.

Dymiotis, C., Kappos, A. J., and Chryssanthopoulos, M. K., 2001. Seismic reliability of masonry-infilled RC frames. *Journal of Structural Engineering*, 127(3), 296–305.

Eberhard, M. O., Baldridge, S., Marshall, J., Mooney, W., and Rix, G. J., 2013. *Mw 7.0 Haiti Earthquake of January 12, 2010: Usgs/eeri Advance Reconnaissance Team Report*, USGS, Reston. VA.

EERI., 1999. *Learning from Earthquakes, The Izmit (Kocaeli), Turkey Earthquake of August 17, 1999, Oakland, CA*.

Elwood, K. J., 2004. Modelling failures in existing reinforced concrete columns. *Canadian Journal of Civil Engineering*, 31(5), 846–859.

Faison, H., Comartin, C., and Elwood, K., 2004. *Reinforced concrete moment frame building without seismic details*. *www.world-housing.net*.

Fardis, M. N., 1996. *Experimental and numerical investigations on the seismic response of RC infilled frames and recommendations for code provisions*. . ECOEST/PREC 8, Report No. 6, LNEC, Lisbon.

FEMA., 1998. *Evaluation of Earthquake Damaged Concrete and Masonry Wall Buildings*. Applied Technology Council, Redwood City, CA.

FEMA., 2009. *Quantification of Building Seismic Performance Factors (FEMA P695).*, Prepared by ATC for FEMA , Washington (DC).

Fiorato, A. E., Sozen, M. A., and Gamble, W. L., 1970. *An investigation of the interaction of reinforced concrete frames with masonry filler walls*. Dept. of Civil Engineering, University of Illinois, Urbana- Champaign, IL.

Flanagan, R. D., and Bennett, R. M., 1999. Arching of masonry infilled frames: comparison of analytical methods. *Practice Periodical on Struc. Des. and Construc.*, 4(3), 105–110.

Gabrielsen, B. L., and Kaplan, K., 1997. Arching in masonry walls subjected to out-of-plane forces. *Earthquake Resistant Masonry Construction, NBS Building Science Series*, 106, 283–313.

Hamburger, R. O., and Meyer, J. D., 2006. The performance of steel-frame buildings with infill masonry walls in the 1906 San Francisco earthquake. *Earthquake Spectra*, 22(S2), 43–67.

Haselton, C. B., Liel, A. B., Lange, S. T., and Deierlein, G. G., 2008. *Beam-Column Element Model Calibrated for Predicting Flexural Response Leading to Global Collapse of RC Frame Buildings,* PEER Rep. 2007/03, CA, Berkeley.

Haselton, C., Baker, J., Liel, A., and Deierlein, G., 2011. Accounting for ground-motion spectral shape characteristics in structural collapse assessment through an adjustment for epsilon. *Journal of Structural Engineering*, 137(3), 332–344.

Hashemi, A., and Mosalam, K., 2007. *Seismic evaluation of reinforced concrete buildings including effects of masonry infill walls*. PEER Rep.2007/100, CA, Berkeley.

Holmes, W. T., Mehrain, M., and Sommers, P., 2013. *Personal communication*.

Ibarra, L., Medina, R., and Krawinkler, H., 2005. Hysteretic models that incorporate strength and stiffness deterioration. *Journal of Earthquake Engineering and Structural Dynamics*, 34, 1489–1511.

ICBO., 1927. *Uniform Building Code*. Long Beach, CA.

ICBO., 1997. *Uniform Building Code*. Long Beach, CA.

Kam, W. Y., Pampanin, S., Dhakal, R. P., Gavin, H., and Roeder, C. W., 2010. Seismic performance of RC buildings in the September 2010 Darfield (Canterbury) earthquakes. *Bull. of New Zealand Soc. of Earthquake Eng*, 43(4), 340–350.

Kariotis, J., 1991. *Determination of the Compressive Modulus of Masonry by Use of Flat-Jacks*. San Pedro Masonry Infill Evaluation, Los Angeles, CA.

Lee, H.-S., and Woo, S.-W., 2002. Effect of masonry infills on seismic performance of a 3-storey R/C frame with non-seismic detailing. *Earthquake Engineering & Structural Dynamics*, 31(2), 353–378.

Li, X., Zhou, Z., Yu, H., Wen, R., Lu, D., Huang, M., Zhou, Y., and Cu, J., 2008. Strong motion observations and recordings from the great Wenchuan Earthquake. *Earthquake Engineering and Engineering Vibration*, 7(3), 235–246.

Liel, A. B., Haselton, C. B., and Deierlein, G. G., 2011. Seismic collapse safety of reinforced concrete buildings. II: comparative assessment of nonductile and ductile moment frames. *Journal of Structural Engineering*, 137(4), 492–502.

Liel, A. B., and Lynch, K. P., 2012. Vulnerability of RC frame buildings and their occupants in the 2009 L'Aquila, Italy, earthquake. *Natural Hazards Review*, 13(1), 11–23.

Linares, J. G., 2007. Adaptive Reuse of Existing Structures. *Structure magazine*, 26–27.

Lotfi, H. R., and Shing, P. B., 1994. Interface model applied to fracture of masonry structures. *Journal of Structural Engineering*, 120(1), 63–80.

Lourenco, P., 1996. Computational Strategies for Masonry Structures. Ph.D. Thesis, Universidade do Porto, Portugal.

Madan, A., and Hashmi, A. K., 2008. Analytical prediction of the seismic performance of masonry infilled reinforced concrete frames subjected to near-field earthquakes. *Journal of Structural Engineering*, 134(9), 1569–1581.

Maheri, M. R., 1990. Engineering aspects of the Manjil, Iran earthquake of 20 June 1990. *A field report by EEFIT, Earthquake Eng. Field Investigation Team (EEFIT), London*.

Mehrabi, A., 1994. Behavior of Masonry-Infilled Reinforced Concrete Frames Subjected to Lateral Loading. Ph.D. Thesis, University of Colorado-Boulder, CO.

Mehrabi, A. B., Benson Shing, P., Schuller, M. P., and Noland, J. L., 1996. Experimental evaluation of masonry-infilled RC frames. *Journal of Structural Engineering*, 122(3), 228–237.

Moehle, J. P., 2003. Assessment of the collapse of a concrete frame intended to meet US seismic requirements. *5th US-Japan Workshopon Performance-Based Earthquake Engineering for Reinforced Concrete Building Structures*, Hakone, Japan.

Moehle, J. P., Ghannoum, W., and Bozorgnia, Y., 2006. Collapse of lightly confined concrete frames during earthquakes. *Advances in Earthquake Engineering for Urban Risk Reduction*, Nato Science Series: IV: Earth and Environmental Sciences, S. T. Wasti and G. Ozcebe, eds., Springer Netherlands, 317–332.

Nakamura, H., and Higai, T., 2001. Compressive fracture energy and fracture zone length of concrete. *Modeling of Inelastic behavior of RC Structures under Seismic Loads*, ASCE, 471–487.

Pestana, J. M., Mendoza, M. J., Mayoral, J. M., Moss, E. S., Sancio, R. B., Seed, R. B., Bray, J. D., and Romo, M. P., 1999. *Preliminary Report on the Geotechnical Engineering Aspects of the June 15 and June 21, 1999, Mexico,'Earthquakes of the Churches'*., Dep. of Civil and Environmental Engineering, University of California, Berkeley.

Rao, G. A., 2001. Generalization of Abrams' law for cement mortars. *Cement and Concrete Research*, 31(3), 495–502.

Rossetto, T., and Elnashai, A., 2003. Derivation of vulnerability functions for European-type RC structures based on observational data. *Engineering Structures*, 25(10), 1241–1263.

Sattar, S., 2013. Influence of Masonry Infill Walls and Other Building Characteristics on Seismic Collapse of Concrete Frame Buildings. Ph.D. Thesis, University of Colorado-Boulder, CO.

Sattar, S., and Liel, A., 2014. Seismic performance of non-ductile reinforced concrete frames with masonry infill walls: I. Development of a finite element enhanced strut modeling approach., submitted.

Sattar, S., and Liel, A. B., 2010. Seismic performance of reinforced concrete frame structures with and without masonry infill walls. *9th US National and 10th Canadian Conference on Earthquake Engineering, Toronto, Canada*.

Schmid, B., Kariotis, J., and Schwartz, E., 1978. Tentative Los Angeles ordinance and testing program for unreinforced masonry buildings. Proc. of the 47th Annual Convention of the Structural Engineers Association of California, South Lake Tahoe.

Sezen, H., and Moehle, J., 2004. Shear strength model for lightly reinforced concrete columns. *Journal of Structural Engineering*, 130(11), 1692–1703.

Sezen, H., Whittaker, A. S., Elwood, K. J., and Mosalam, K. M., 2003. Performance of RC buildings during the August 17, 1999 Kocaeli, Turkey earthquake, and seismic design and construction practice in Turkey. *Engineering Structures*, 25(1), 103–114.

Shing, P. B., 2013. Collapse simulation of masonry-infilled RC frames. ATC-95 workshop on Collapse Simulation, San Francisco, CA.

Stang, A. H., Parsons, D. E., and McBurney, J. W., 1929. Compressive strength of clay brick wall. Bureau of Standards Journal of Research, 3(108), 507–571.

Stavridis, A., 2009. Analytical and Experimental Study of Seismic Performance of Reinforced Concrete Frames Infilled with Masonry Walls. Ph.D. Thesis, University of California San Diego, CA.

Stavridis, A., Koutromanos, I., and Shing, P. B., 2012. Shake-table tests of a three-story reinforced concrete frame with masonry infill walls. *Earthquake Engineering & Structural Dynamics*, 41(6), 1089–1108.

Thomas, F. G., 1953. The strength of brickwork. The Structural Engr., London; 31:35-47.

Tothong, P., and Luco, N., 2007. Probabilistic seismic demand analysis using advanced ground motion intensity measures. *Earthquake Engineering & Structural Dynamics*, 36(13), 1837–1860.

Turneaure, F. E., and Maurer, E. R., 1914. *Principles of Reinforced Concrete Construction*. John Wiley & Sons, Inc., New York.

Turneaure, F. E., and Maurer, E. R., 1935. *Principles of Reinfroced Concrete Construction*. John Wiley & Sons, Inc., New York.

Vamvatsikos, D., and Cornell, C. A., 2002. Incremental dynamic analysis. *Earthquake Engineering & Structural Dynamics*, 31(3), 491–514.

Van der Pluijm, R., 1992. Material properties of masonry and its components under tension and shear. *Proceedings of the 6 th Canadian Masonry Symposium. Saskatoon, University of Saskatchewan*.

Wittmann, F. H., 2002. Crack formation and fracture energy of normal and high strength concrete. *Sadhana*, 27(4), 413–423.

Zarnic, R., and Tomazevic, M., 1988. An experimentally obtained method for evaluation of the behavior of masonry infilled RC frames. *Proceedings of the 9th World Conference on Earthquake Engineering*, 163–168.

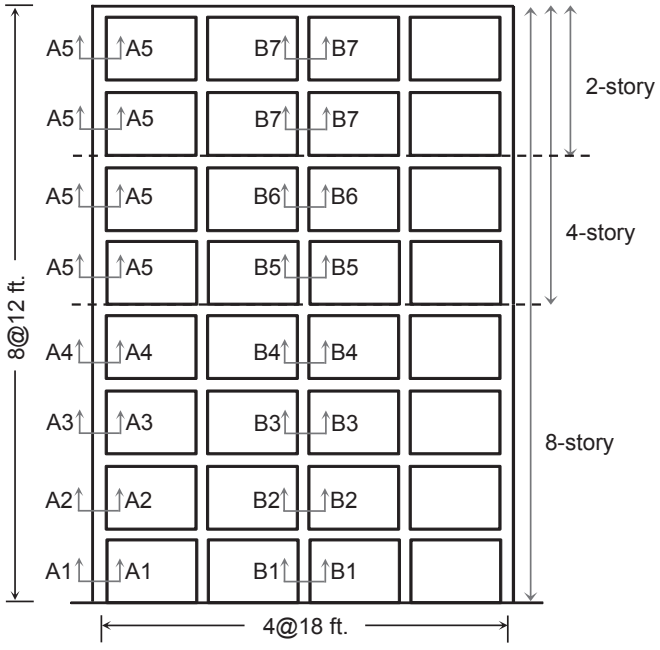

Section	Dimensions	Longitudinal Reinforcement	Tie
A1-A1	24"x24"	8#8	#3@8"
B1-B1	26"x26"	8#8	#3@8"
A2-A2	22"x22"	6#8	#3@8"
B2-B2	26"x26"	8#8	#3@8"
A3-A3	20"x20"	6#8	#3@8"
B3-B3	24"x24"	8#8	#3@8"
A4-A4	18"x18"	6#8	#3@8"
B4-B4	22"x22"	8#8	#3@8"
A5-A5	16"x16"	6#8	#3@8"
B5-B5	18"x18"	6#8	#3@8"
B6-B6	16"x16"	4#8	#3@8"
B7-B7	14"x14"	4#8	#3@8"

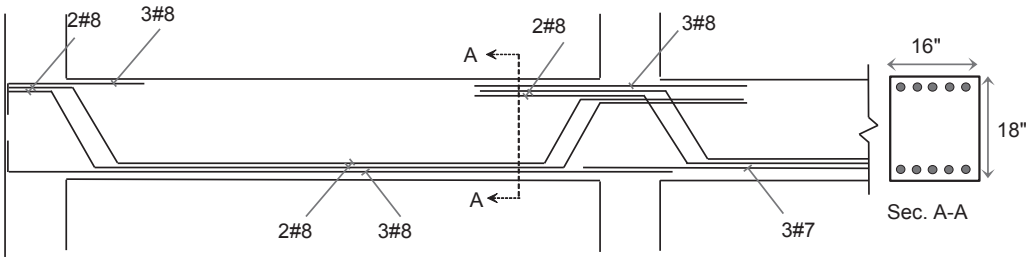
2#8
3#8
A
2#8
3#8
16"
18"
A
2#8
3#8
3#7
Sec. A-A

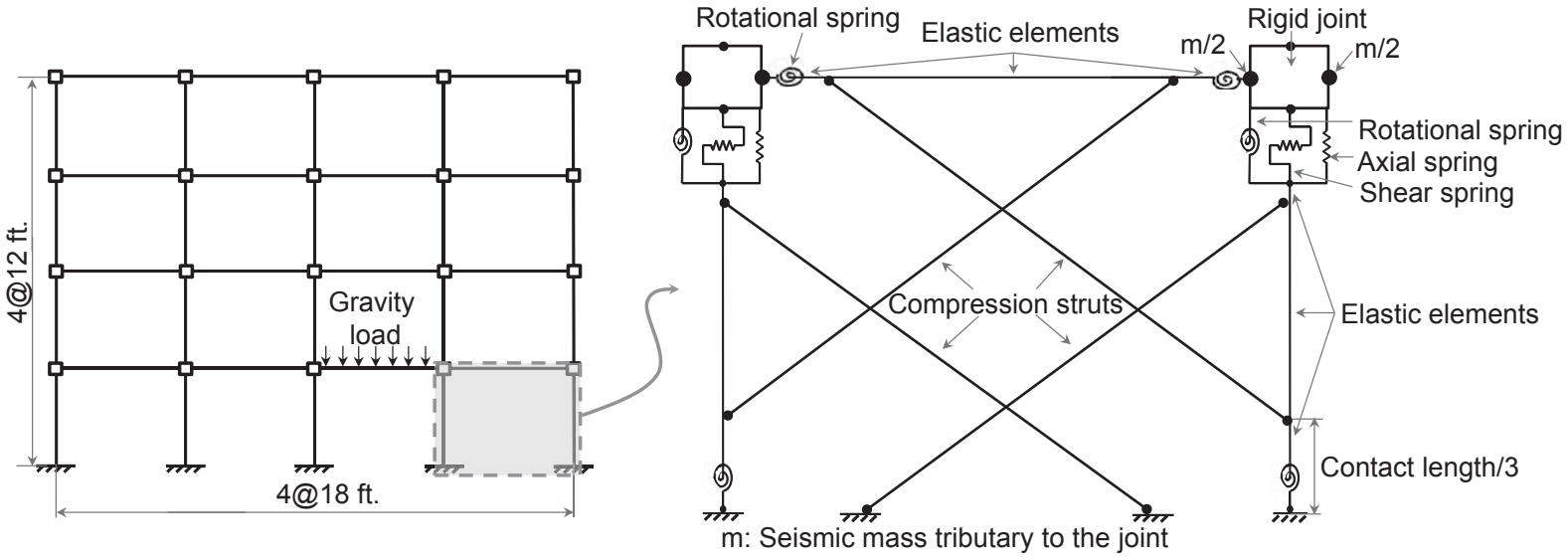
4@12 ft.
Gravity load
4@18 ft.
Rotational spring
Elastic elements
m/2
Rigid joint
m/2
Rotational spring
Axial spring
Shear spring
Compression struts
Elastic elements
Contact length/3
m: Seismic mass tributary to the joint

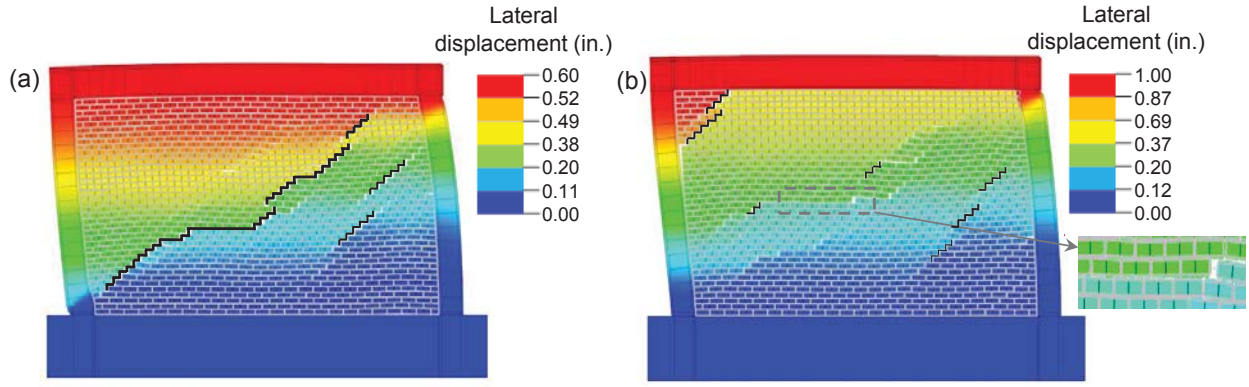
(a)
Lateral displacement (in.)
0.60
0.52
0.49
0.38
0.20
0.11
0.00
(b)
Lateral displacement (in.)
1.00
0.87
0.69
0.37
0.20
0.12
0.00

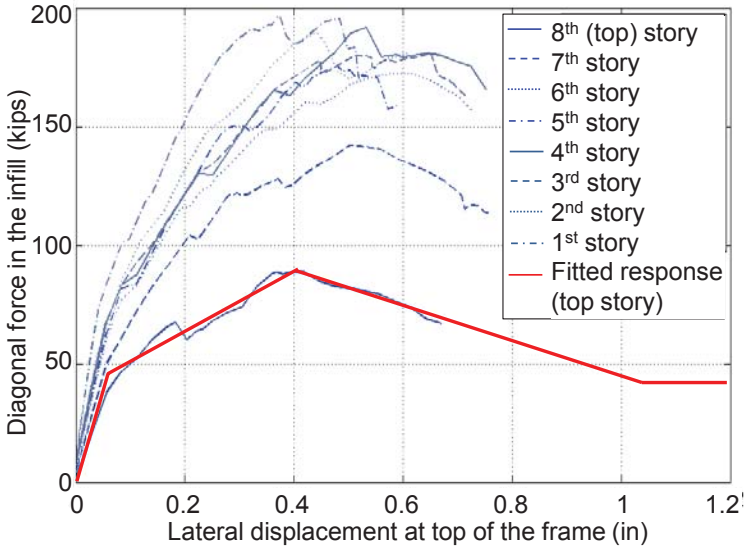
Diagonal force in the infill (kips)
Lateral displacement at top of the frame (in)
0
50
100
150
200
0
0.2
0.4
0.6
0.8
1
1.2
8th (top) story
7th story
6th story
5th story
4th story
3rd story
2nd story
1st story
Fitted response (top story)

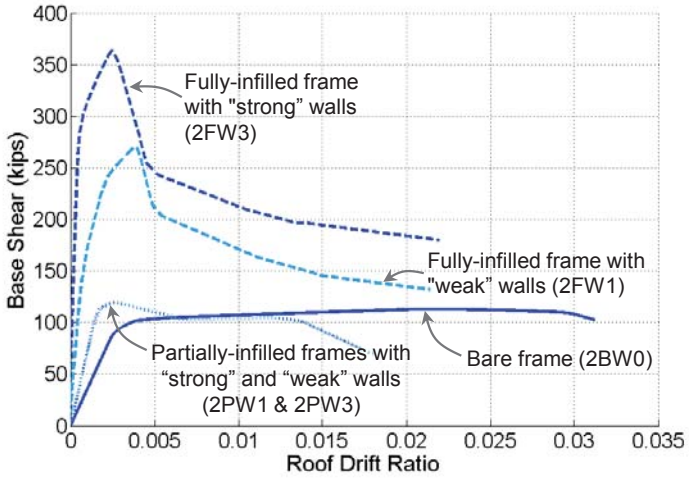
Base Shear (kips)
Roof Drift Ratio
400
350
300
250
200
150
100
50
0
0
0.005
0.01
0.015
0.02
0.025
0.03
0.035
Fully-infilled frame with "strong" walls (2FW3)
Fully-infilled frame with "weak" walls (2FW1)
Partially-infilled frames with "strong" and "weak" walls (2PW1 & 2PW3)
Bare frame (2BW0)

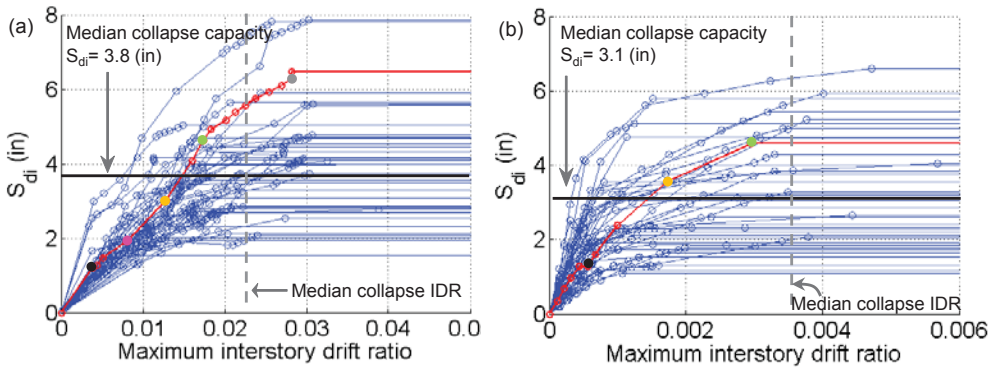
(a)
Median collapse capacity
S_{di}= 3.8 (in)
Median collapse IDR
S_{di} (in)
Maximum interstory drift ratio
0
2
4
6
8
0.01
0.02
0.03
0.04
0.0
(b)
Median collapse capacity
S_{di}= 3.1 (in)
Median collapse IDR
S_{di} (in)
Maximum interstory drift ratio
0.002
0.004
0.006

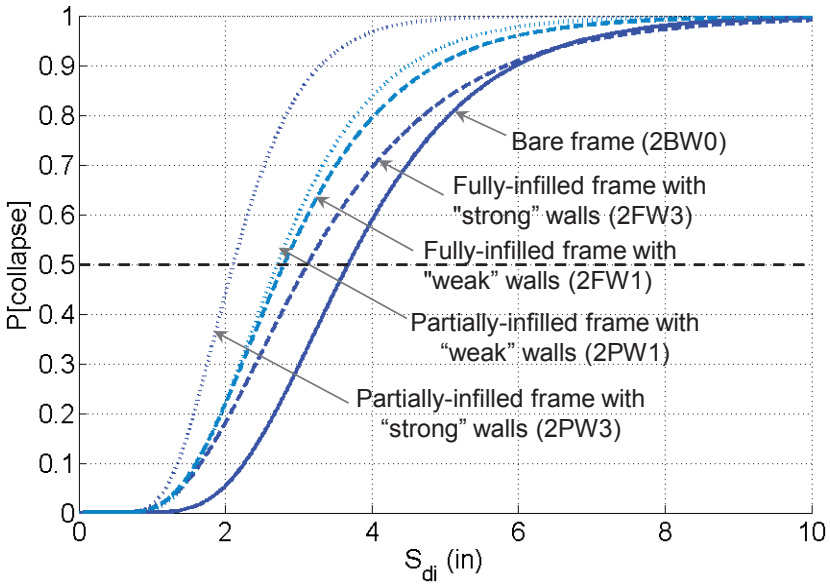
P[collapse]
1
0.9
0.8
0.7
0.6
0.5
0.4
0.3
0.2
0.1
0
0
2
4
6
8
10
S_di (in)
Bare frame (2BW0)
Fully-infilled frame with "strong" walls (2FW3)
Fully-infilled frame with "weak" walls (2FW1)
Partially-infilled frame with "weak" walls (2PW1)
Partially-infilled frame with "strong" walls (2PW3)

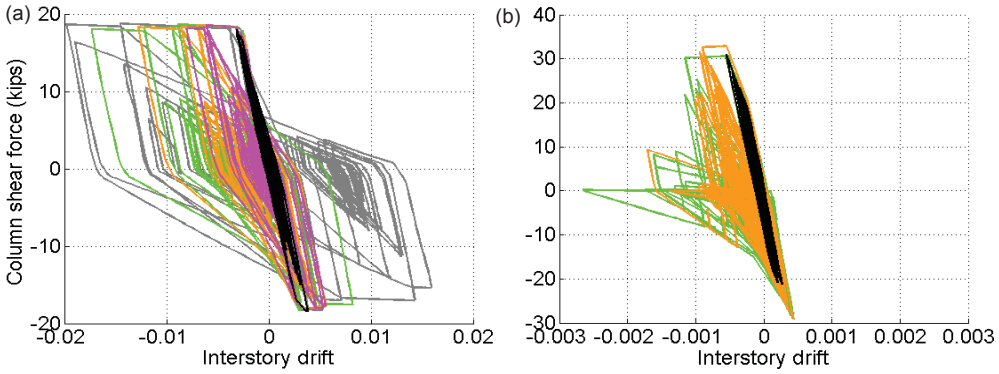
(a)
(b)
Column shear force (kips)
Interstory drift
Interstory drift
20
10
0
-10
-20
-0.02
-0.01
0
0.01
0.02
40
30
20
10
0
-10
-20
-30
-0.003
-0.002
-0.001
0
0.001
0.002
0.003

(a)

(b)